Hyperspherical-coordinate approach to one-dimensional models of two-electron quantum systems

A. Artemyev,* R. Grobe, and J. H. Eberly
Department of Physics and Astronomy, University of Rochester, Rochester, New York 14627
(Received 2 September 1994)

The applicability and accuracy of the hyperspherical-coordinate method for the study of reduced-dimensional models of two-electron atoms and ions is discussed. We have calculated excitation spectra and ground-state wave functions and compared them with their exact values, and with the values obtained within different modifications of the Hartree-Fock approach.

PACS number(s): 31.15.Ar, 31.25.−v, 31.15.Ja

I. INTRODUCTION

The theoretical treatment of multielectron systems is a problem of central interest in atomic physics. Most of our current understanding of the structure and behavior of atomic systems stems from models which regard each electron as moving in the combined field of the nucleus and the average field of the other electrons. A sequence of approaches has been developed to deal with interactions and correlated behavior of atomic electrons. One of them is the use of the Slater determinant introducing the "Pauli correlations" which result from the indistinguishability of electrons. Correlated atomic electrons can be described by superimposing wave functions constructed from independent-electron models with coefficients that stabilize the mean value of the Hamiltonian under first-order perturbations. Various kinds of such variational wave functions have been used extensively to obtain information about two-electron energy levels and autoionization rates [1].

One consequence of electron correlation in helium was discovered in 1963 in the observation of the series of doubly excited $^1P_0$ levels by Madden and Codling [2]. These results were first understood in terms of linear combinations of $2snp$ and $2pns$ excited states by Cooper, Fano, and Prats [3], and in more detail by other authors later [4]. Significant progress was made in 1968 when Macek suggested an alternative way to study the correlated behavior of the two helium electrons by introducing the hyperspherical basis [5]. He explained the observed large differences of brightness and spectral width of various Rydberg series, and unified the results of previous investigations within his approach. Later the hyperspherical method was applied to the study of three-particle scattering problems [6]. Recent work using the hyperspherical approach to study two-electron systems has been devoted to the behavior of the wave functions at large distances, the estimation of errors due to nonadiabaticity, and the study of the analytic properties of the wave functions in the vicinity of adiabatic level crossings [7]. Extensive lists of references can be found in review articles by Fano [8] and Lin [9].

There are rather few studies [10,11] that apply the hyperspherical method to the interaction of two-electron systems with electromagnetic radiation. Klar, Zoller, and Fedorov [10] showed how adiabatic potential curves can be modified by laser light and predicted field-dressed two-electron states. Abrashkevich and Shapiro [11] used an artificial-channel method in the hyperspherical basis to calculate the photoionization cross sections for the negative hydrogen ion and for helium.

Reduced-dimension studies represent another way to explore the complexity of two-electron quantum systems. Such studies have been inspired by the possibility to solve numerically the full time-dependent Schrödinger equation. Although the full three-dimensional (3D) problem is beyond the capability of today's computers, important information about the behavior of 3D systems can be extracted from the analysis of their 1D analogs. Reduced-dimensional systems resemble in many of their features the corresponding 3D systems and reproduce qualitatively the dynamical properties of their 3D analogs. On the other hand, reduced-dimension analysis cannot recover those properties of the 3D system that depend crucially on the angular degrees of freedom.

One-dimensional models have the strong advantage that exact fully correlated wave functions can be computed numerically [12], and this allows for an unambiguous test of the accuracy of approximation schemes [13]. The effects of single and double ionization of two-electron atoms driven by strong fields have also been successfully investigated both quantum mechanically [14,15] and classically [16,17]. Methods which combine classical and quantum-mechanical descriptions have been proposed to describe the ionization of multielectron systems [18]. Information about the structure of highly excited states [19] and the dynamical behavior of autoionizing decay [20] have been used to check the applicability of various types of Hartree-Fock methods [13,20]. Some studies have led to the discovery of phenomena [21] based on strong electron-electron correlation, and to measures for the de-

*Permanent address: General Physics Institute, Russian Academy of Sciences, Vavilov Street 38, 117942 Moscow, Russia.

gree of electron-electron correlation [22].

The hyperspherical approach applied to two-electron atoms does not have a well-defined small parameter justifying the approach *a priori* as in the related Born-Oppenheimer approximation for molecules. However, the hyperspherical approach has provided one of the major theoretical frameworks in atomic physics for the calculation of bare energies, states, and oscillator strengths of multielectron systems. Its success in three spatial dimensions is based on the large difference between the corresponding time scales for the fast interelectron motion and the slow collective motion described by the hyperradius. It provides a natural framework for classification schemes of singly and doubly excited states [9].

In this paper we investigate whether the hyperspherical approach can be applied to reduced-dimensional systems as well. We describe the static properties of 1D two-electron systems and compare the energy-level positions found within the hyperspherical approach with their exact values and also with values found from different kinds of Hartree-Fock approximations. We find that the hyperspherical approximation works remarkably well even in one spatial dimension.

II. THE MODEL AND THE HYPERSPHERICAL COORDINATE APPROXIMATION

Let us begin with a brief description of our two-electron system. It is characterized by a nucleus of positive charge Z fixed at the origin at $x=0$ and two electrons whose spatial coordinates are x_1 and x_2. Its bare Hamiltonian is (in atomic units, a.u.)

$$H(x_1,x_2)=\frac{p_1^2}{2}+\frac{p_2^2}{2}+ZV(x_1)+ZV(x_2)-V(x_1-x_2)\ , \tag{2.1}$$

where the soft-core Coulomb potential has been chosen as

$$V(y)=-\frac{1}{\sqrt{y^2+1}}\ . \tag{2.2}$$

This potential has been studied extensively in the one-electron context, mostly for strong laser interactions [23], and its behavior has proved remarkably useful. In the present case it permits the two electrons to move past the nucleus and past each other so the entire x axis is available for both electrons. In Fig. 1(a) we show the total two-electron potential as a function of coordinates x_1 and x_2. The spine along the line $x_1=x_2$ indicates that it is energetically not favored to find both electrons on the same side of the nucleus. The potential, and thus the bare Hamiltonian, is invariant under the two symmetry operations:

$$H(x_1,x_2)=H(-x_1,-x_2),\quad H(x_1,x_2)=H(x_2,x_1)\ . \tag{2.3}$$

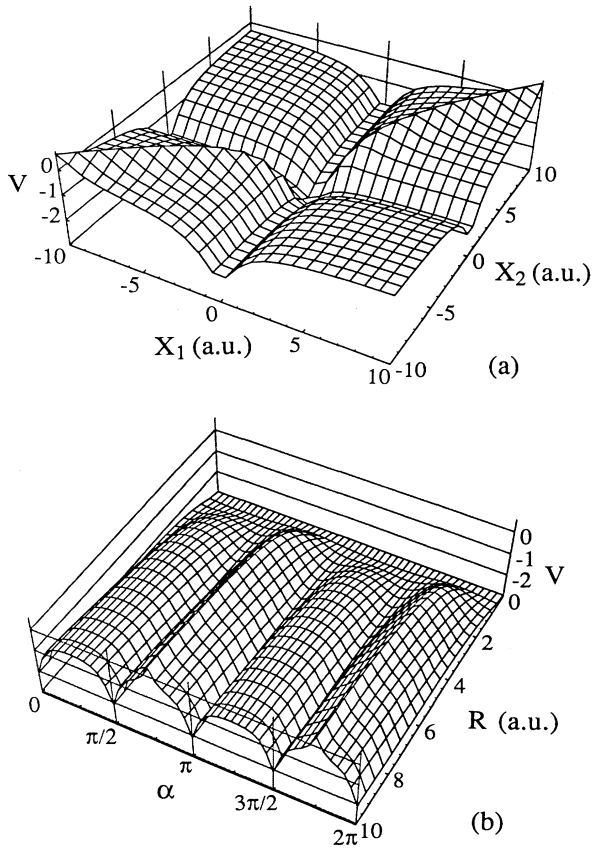

FIG. 1. The total two-electron potential $V(x_1,x_2)=ZV(x_1)+ZV(x_2)-V(x_1-x_2)$ as defined in Eq. (2.1) (a) as a function of electron coordinates x_1 and x_2; and (b) as a function of the hyperspherical coordinates R and α.

The energy eigenstates can be classified as having a different spatial parity or being even or odd with respect to the permutation of both electron coordinates:

$$\Psi(x_1,x_2)=\pm\Psi(-x_1,-x_2)\ ,\qquad \Psi(x_1,x_2)=\pm\Psi(x_2,x_1)\ . \tag{2.4}$$

Thus the time-independent Schrödinger equation for the energies and eigenfunctions can be decomposed into four independent subspaces. This property is important for the applicability of the hyperspherical method described below.

We introduce the hyperspherical coordinates R and α:

$$R\equiv\sqrt{(x_1^2+x_2^2)}\ \text{ and }\ \tan\alpha\equiv x_1/x_2\ , \tag{2.5}$$

where the hyperangle α describes the ratio of the distances from the nucleus to the electrons. Note that in the one-dimensional case these coordinates are identical to the usual polar coordinates with the angle α ranging from 0 to 2π. The hyperspherical coordinates are collective coordinates for the electron pair and thus they are convenient for the description of strong electron-electron correlation. In fact the Hamiltonian in hyperspherical

coordinates is quasiseparable as is its analog in three spatial dimensions. This corresponds to a slow motion along the R coordinate and a relatively faster motion along the α coordinate. The Hamiltonian (2.1) for the two electrons then reads

$$H=-\frac{1}{2}\left[\frac{\partial^2}{\partial R^2}+\frac{1}{R}\frac{\partial}{\partial R}+\frac{1}{R^2}\frac{\partial^2}{\partial\alpha^2}\right]+V(R,\alpha)\ , \quad (2.6)$$

where $V(R,\alpha)\equiv ZV(R\cos\alpha)+ZV(R\sin\alpha)-V(R\cos\alpha-R\sin\alpha)$. The potential $V(R,\alpha)$ is displayed in Fig. 1(b). Note that for small R the potential becomes independent of α, and for large values of R it develops into a characteristic shape with four minima. After the substitution $\Phi(R,\alpha)\equiv R^{1/2}\Psi(R,\alpha)$ the corresponding Hamiltonian takes a simplified form, with the kinetic part containing only second derivatives in R and α:

$$H\Phi(R,\alpha)=\left[-\frac{1}{2}\frac{\partial^2}{\partial R^2}+H_\alpha\right]\Phi(R,\alpha)=E\Phi(R,\alpha)\ , \quad (2.7)$$

where the angular Hamiltonian H_α is defined as

$$H_\alpha\equiv\frac{1}{R^2}\left[-\frac{1}{2}\frac{\partial^2}{\partial\alpha^2}-\frac{1}{8}+R^2V(R,\alpha)\right]\ . \quad (2.8)$$

The stationary Schrödinger equation can be solved approximately by an ansatz:

$$\Phi(R,\alpha)=f(R)\varphi(R,\alpha)\ . \quad (2.9)$$

If we insert this expression into the Schrödinger equation, we obtain

$$-\tfrac{1}{2}\varphi(R,\alpha)\frac{\partial^2}{\partial R^2}f(R)+f(R)[H_\alpha-E]\varphi(R,\alpha)=\left[\frac{1}{2}\frac{\partial^2}{\partial R^2}\varphi(R,\alpha)-\varphi(R,\alpha)\frac{1}{2}\frac{\partial^2}{\partial R^2}\right]f(R)\ . \quad (2.10)$$

As a first approximation we will assume that the electron dynamics in the R direction is slow, and neglect all derivatives with respect to R in Eq. (2.10). We will treat the hyper-radius R as a frozen parameter not affecting the dynamics in the α coordinate. It suggests that the function $\varphi(R,\alpha)$ is an eigenfunction of the angular Hamiltonian H_α:

$$H_\alpha\varphi_\nu(R,\alpha)=u_\nu(R)\varphi_\nu(R,\alpha)\ , \quad (2.11)$$

where $u_\nu(R)$ denotes the eigenvalues. H_α depends on the "slow" variable R only parametrically, and its spectrum is discrete because of the periodic boundaries $\varphi_\nu(R,\alpha)=\varphi_\nu(R,\alpha+2\pi)$. We assume that the mutually orthogonal states $\varphi_\nu(R,\alpha)$ are normalized to 1 with respect to α for all values of R. Returning to the full Schrödinger equation (2.10), we assume as a second approximation that the commutator on the right-hand side of (2.10) is very small. This is a commonly used approximation in 3D hyperspherical analyses, and it is based on the assumption that $\varphi_\nu(R,\alpha)$ depends on R slowly such that one can set $\partial^2\varphi/\partial R^2\approx 0$ and $\partial\varphi/\partial R\approx 0$, which will be justified below. Then we multiply equation (2.10) with an orthogonal angular basis state $\varphi_\mu(R,\alpha)$, integrate it over α, and Eq. (2.10) simplifies to

$$\left[-\frac{1}{2}\frac{\partial^2}{\partial R^2}+u_\mu(R)\right]f_{\mu m}(R)=E_{\mu m}f_{\mu m}(R)\ , \quad (2.12)$$

where $E_{\mu m}$ and $f_{\mu m}(R)$ are the eigenenergies and eigenfunctions. As usual, the eigenvalue $u_\mu(R)$ of the Hamiltonian H_α plays the role of an effective potential for Schrödinger's equation in the radial direction. For this reason each eigenvalue of the angular Hamiltonian H_α serves as a "potential curve" for the slow motion in the radial coordinate. The energies $E_{\mu m}$ of the effective one-particle Hamiltonian (2.12) are approximate values for the energies of the original two-electron system (2.1).

We have computed potential curves $u_\mu(R)$ from (2.11) by numerically diagonalizing H_α on an angular grid with periodic boundaries for 400 different values of radius R. Potential curves for two-electron systems are qualitatively quite similar for nuclear charges $Z=1,2,\ldots,5$. We present in Figs. 2(a) and 2(b) the first few lowest-lying curves for the 1D negative hydrogen ion ($Z=1$) and the 1D helium atom ($Z=2$).

Let us discuss the structure of these potential curves. For small values of R the lowest potential curve approaches minus infinity, while the other potentials tend to plus infinity in pairs. For large values of R the curves bunch into groups of four which approach the energies of the corresponding core system (the He^+ ion in the case of $Z=2$). This behavior can be understood by analyzing

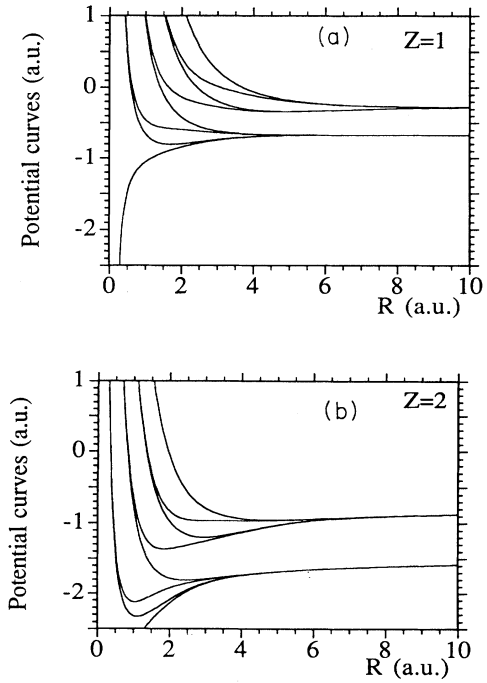

FIG. 2. The lowest-lying potential curves for the negative hydrogen ion and for the He atom: (a) the whole set of potential curves for the negative hydrogen ion; (b) the whole set of potential curves for the He atom.

the symmetry and asymptotic properties of the Hamiltonian H_α.

For small R the angular Hamiltonian H_α multiplied by R^2 tends to the sum of the α-kinetic energy operator plus a constant negative potential:

$$R^2 H_\alpha \to -\frac{1}{2}\frac{\partial^2}{\partial\alpha^2} - \frac{1}{8} \quad (R \to 0) . \tag{2.13}$$

Its spectrum is purely discrete due to the required periodicity of the eigenfunctions. The lowest eigenvalue is $e_1 = \frac{1}{8}$, and all other eigenenergies are pairwise degenerate: $e_{2\nu} = e_{2\nu+1} = \frac{1}{2}\nu^2 - \frac{1}{8}$ (for $\nu = 1,2,3,\ldots$). Correspondingly, the eigenenergies of H_α tend to plus or minus infinity as $R \to 0$:

$$u_1(R) \to -\frac{1}{8R^2} , \quad u_{2\nu}(R) \sim u_{2\nu+1}(R) \to \frac{\nu^2/2 - 1/8}{R^2}$$
$$(\text{for } \nu = 1,2,3,\ldots) . \tag{2.14}$$

For large R the spectrum of H_α is fourfold degenerate. This is due to the fact that the effective potential in $R^2 H_\alpha$ has four minima, each of them corresponding to one of the two electrons close to the nucleus [see Fig. 1(b)]. The depth of these valleys tends to infinity with an increase of radius R, corresponding to the fact that one of the electrons is localized near the nucleus while the other one is far away. The angular wave function can be localized in any of these valleys and, as they become deeper with increasing of R, the fourfold degeneracy of the levels becomes apparent. In the limit $R \to \infty$ the functions $u_\nu(R)$ converge to the ionization thresholds. This can be seen by rewriting H_α in terms of a variable $y \equiv \alpha R$, and assuming a large R while leaving y finite. In this limit H_α becomes $p^2/2 + V(y)$, which describes the core-electron system in the absence of the other electron. Its bound-state energies are exactly the ionization thresholds of the corresponding two-electron system.

III. CLASSIFICATION OF BARE ENERGIES AND EIGENSTATES

As we have mentioned above, the eigenstates can be classified as having different spatial parity and symmetry with respect to electron permutation, as in (2.4). A corresponding classification is also possible for the potential curves. In our (R,α) basis the action of the parity operator $(x_1,x_2) \to (-x_1,-x_2)$ corresponds to the change $\alpha \to \alpha + \pi$, and the electron permutation $(x_1,x_2) \to (x_2,x_1)$ is equivalent to the substitution $\alpha \to \pi/2 - \alpha$. The potential $V(R,\alpha)$ is invariant under both transformations. The symmetries of the eigenfunctions $\varphi_\nu(R,\alpha)$ alternate with the increase of the state number ν, and therefore with the increase of the state energy $u_\nu(R)$, as follows:

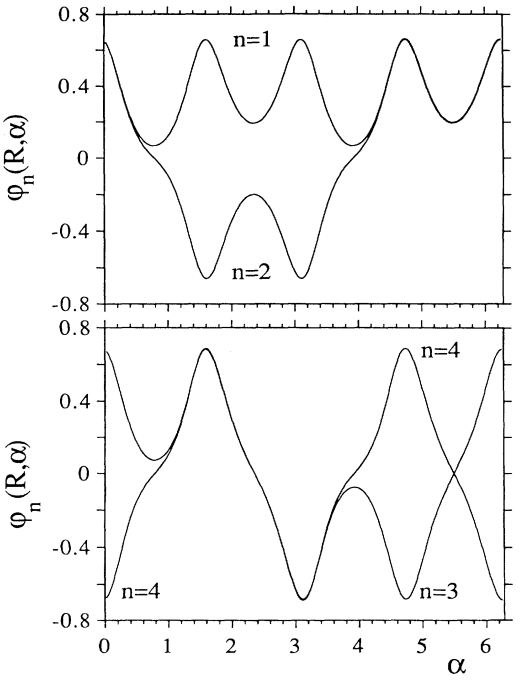

FIG. 3. The first four angular wave functions $\varphi_n(R,\alpha)$. The value of the hyper-radius R is 3.5 a.u.

electron permutation (spin)		spatial parity	
$\varphi_1(R,\alpha) = \varphi_1(R,\pi/2-\alpha)$	and	$\varphi_1(R,\alpha) = \varphi_1(R,\alpha+\pi)$	(3.1a)
$\varphi_2(R,\alpha) = -\varphi_2(R,\pi/2-\alpha)$	and	$\varphi_2(R,\alpha) = -\varphi_2(R,\alpha+\pi)$	(3.1b)
$\varphi_3(R,\alpha) = \varphi_3(R,\pi/2-\alpha)$	and	$\varphi_3(R,\alpha) = -\varphi_3(R,\alpha+\pi)$	(3.1c)
$\varphi_4(R,\alpha) = -\varphi_4(R,\pi/2-\alpha)$	and	$\varphi_4(R,\alpha) = \varphi_4(R,\alpha+\pi)$	(3.1d)

The symmetry properties of every fourth one of the states $\varphi_\nu(R,\alpha)$ are identical. In Fig. 3 we display the four lowest-lying angular wave functions calculated at the radius $R = 3.5$. The energies of the states are determined by the number of zeros they have and by the location of these zeros with respect to the maxima and minima of the potential $V(R,\alpha)$. The state φ_1 has no zeros and has the lowest energy. The states φ_2 and φ_3 have the same number of zeros but their location is different. The state φ_2 is spatially asymmetric and has odd parity, and its zeros are located at $\pi/4$ and $5\pi/4$ where the potential has maxima. On the other hand the state φ_3 has its zeros near

$3\pi/4$ and $7\pi/4$ where the potential $V(R,\alpha)$ has low valleys between its two minima. For these reasons the energy of the odd-parity symmetric state φ_3 is higher than that of the odd-parity asymmetric state φ_2. Analogous arguments classify the higher-lying potential curves as well.

The level classification is relevant in deciding whether the hyperspherical approximation is appropriate for a description of 1D two-electron systems. Indeed, the hyperspherical method described is applicable if the commutator [right-hand side of Eq. (2.10)] can be ignored. The condition for that requires that the energy separation between potential curves is large enough compared to the rate of change of the eigenfunctions $\varphi_\eta(R,\alpha)$ with respect to R:

$$\left\langle \varphi_\eta(R,\alpha) \left| \frac{\partial^2}{\partial R^2} \right| \varphi_\mu(R,\alpha) \right\rangle \ll u_\eta(R) - u_\mu(R) ,$$
$$\left\langle \varphi_\eta(R,\alpha) \left| \frac{\partial}{\partial R} \right| \varphi_\mu(R,\alpha) \right\rangle \ll u_\eta(R) - u_\mu(R) , \tag{3.2}$$

where absolute magnitudes are understood on both sides. The larger the differences between the potential curves $u_\eta(R)$, the better the reliability of the hyperspherical approach. Figure 2 indicates that both at small and large values of R some potential curves become infinitely close to each other. However, this does not lead to inapplicability of our approach because these curves belong to different symmetry classes and cannot interfere with each other. The relevant potential curves that should be taken into account in criterion (3.2) are those whose indices differ by 4. Those curves are indeed well separated and, in contrast to the 3D case, we did not find any avoided level crossings for the lower-lying potential curves.

From now on we will restrict our analysis to spin singlet states corresponding to wave functions that are even under electron permutation. We discard from our discussion every second potential curve and use the labels $n=1,2,3,..$ to enumerate the relevant potential curves $u_n(R)$ from below.

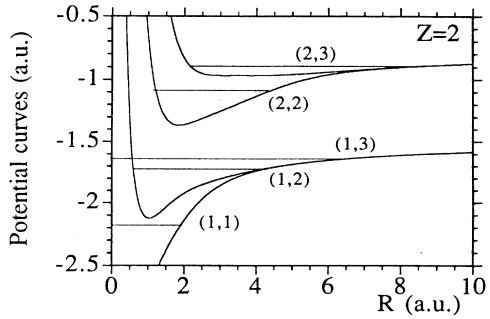

FIG. 4. The relevant lowest-lying He atom potential curves for two-electron wave functions which are even with respect to electron permutation. The energies of the ground state as well as the first few singly and doubly excited states are also presented. We have used independent-electron labels.

In the remaining part of this section we will calculate the hyperspherical energies for a specific reduced-dimensional two-electron system with a rich structure of singly as well as doubly excited states. We will investigate whether the excitation spectrum for 1D helium can be predicted by the hyperspherical method and compare it with its exact values. When substituted into the radial equation, each potential curve $u_n(R)$ provides a set of eigenstates for the total system. Each state is then characterized by the number of the potential curve and by the state number within this particular potential curve (Fig. 4). It is important to note that one can identify some of the states in the hyperspherical picture (n,m) with the states enumerated by two principal quantum numbers (n_1,n_2) in the independent-electron picture ap-

TABLE I. The lowest-lying states of the 1D helium atom. Note that, in general, sharp energies of autoionizing states depend always on details of the approximation scheme used to couple bound states to a continuum. The three autoionizing energies presented here (see the asterisks) were obtained by S. L. Haan from a partitioned Hilbert-space diagonalization approach [20].

Exact energy (a.u.)	Hyperspherical energy (a.u.)	Classification by independent-electron excitations	Potential-curve number	State No. within potential
−2.238	−2.185	(1,1)	1	1
−1.704	−1.725	(1,2)	2	1
−1.626	−1.629	(1,3)	1	2
−1.567	−1.570	(1,4)	2	2
−1.545	−1.542	(1,5)	1	3
−1.483	−1.483	$(1,\infty)$	1 and 2	∞
−1.045*	−1.085	(2,2)	3	1
−0.882*	−0.897	(2,3)	4	1
−0.857*	−0.864	(2,4)	3	2
−0.772	−0.772	$(2,\infty)$	3 and 4	∞

proach. The ground state of the lowest potential curve $u_1(R)$ for 1D helium has an energy -2.185 a.u. and is naturally identified with the (1,1) ground state when both "independent" electrons are not excited. The next eigenenergy generated by the curve $u_1(R)$ corresponds to the second excited state (1,3) with energy -1.629 a.u. Both of these states have even parity as both of them are proportional to the same angular state $\varphi_1(R,\alpha)$. The first excited state is calculated from the potential curve $u_2(R)$. It has an energy -1.725 a.u. and is associated with the state with one single-electron excitation (1,2). The wave function of this state is odd with respect to change of the electron coordinate signs. The second excited state found in the second potential curve $u_2(R)$ corresponds to the (1,4) excitation and its energy is -1.570 a.u.

The first autoionizing state, or in other words the (2,2) state with both electrons excited, corresponds to the lowest state generated by the third potential curve. It has energy equal to -1.085 a.u. The first excited state -0.864 a.u. in the third potential curve would be labeled (2,4). Both of these autoionizing states have positive parity, while the lowest state in the fourth potential curve at -0.897 a.u. was identified with the negative parity state (2,3).

As was mentioned above, the hyperspherical method yields exact values for the ionization thresholds. The potential curves converge at large values of hyper-radius R to the known [20] values of the ionization thresholds. Table I compares the energies obtained within the hyperspherical method with their exact values and with the results of Hartree-Fock calculations and of a partitioned Hilbert space diagonalization approach [20]. This quantitative comparison shows that the hyperspherical method predicts remarkably accurately (error $<5\%$) the excitation spectrum for the helium atom even in reduced dimension. This accuracy is especially surprising in view of the fact that in 1D the hyperspherical coordinates reduce to simple polar coordinates.

IV. GROUND-STATE ENERGIES AND WAVE FUNCTIONS OBTAINED FROM VARIOUS APPROXIMATION METHODS

In this section we present the ground-state wave functions and energies as computed according to three different approximation techniques. We focus on a comparison of the approximate ground-state energies and wave functions with the exact ones obtained from direct numerical computations.

Table II summarizes our results for the ground-state energies of the first five ions of the isoelectronic series beginning with H^-. The second column shows the energy obtained from the hyperspherical coordinate approach discussed in Sec. II. The third column reproduces the energies obtained from the Hartree-Fock (HF) approach in which the functional form of the wave function is restricted to a product of two identical single-electron orbitals: $\Psi(x_1,x_2)=g(x_1)g(x_2)$. The fourth column is obtained from an approximation method which is similar to the traditional HF method, but the product wave functions are different and presented in the hyperspherical coordinates: $\Psi(x_1,x_2)=R^{-1/2}F(R)G(\alpha)$. The questions are whether this combination of hyperspherical coordinates can lead to better results than traditional HF calculations and how these two methods, the hyperspherical method and the exact calculations, are related to each other.

TABLE II. Ground-state energies (a.u.) of the isoelectronic series of 1D two-electron ions beginning with H^-.

	Energy levels			
Nuclear charge	Exact	Hyperspherical	Hartree-Fock[a] x_1,x_2	Hartree-Fock R,α
$Z=1$	-0.731	-0.726	-0.692	-0.656
$Z=2$	-2.238	-2.185	-2.224	-2.132
$Z=3$	-3.896	-3.797	-3.888	-3.752
$Z=4$	-5.615	-5.472	-5.610	-5.437
$Z=5$	-7.371	-7.187	-7.367	-7.162

[a]Values from Refs. [12] and [20].

The ground states and their energies for both versions of the HF method have been found by imaginary time integration of the HF equations. The equations of motion for the HF wave functions $F(R)$ and $G(\alpha)$ were found by minimizing the time-dependent Raleigh-Ritz functional for the HF wave functions $F(R)$ and $G(\alpha)$ were found by minimizing the time-dependent Rayleigh-Ritz functional [24]. The general procedure for finding these equations is as follows. Typically, the two-electron Hamiltonian has the form $H_x+H_y+V_{x,y}$ and the HF approach requires us to minimize the following functional:

$$\langle f(x)g(y)|\left[-i\frac{\partial}{\partial t}+H_x+H_y+V_{x,y}\right]|f(x)g(y)\rangle\ . \quad (4.1)$$

We used two modifications of the HF method, with x and y being either the usual electron coordinates x_1 and x_2 [20] or hyperspherical coordinates R and α. In the second case the resulting equations of motion for $\Psi(R,\alpha)=R^{-1/2}F(R)G(\alpha)$ are

$$i\frac{\partial}{\partial t}F(R)=-\frac{1}{2}\frac{\partial^2}{\partial R^2}F(R)+\langle G(\alpha)|V(R,\alpha)|G(\alpha)\rangle F(R)\ , \quad (4.2)$$

$$i\frac{\partial}{\partial t}G(\alpha)=-\frac{1}{2}\langle F(R)|R^{-2}|F(R)\rangle\frac{\partial^2}{\partial\alpha^2}G(\alpha)+\langle G(\alpha)|V(R,\alpha)|G(\alpha)\rangle F(R)\ .$$

They have been integrated numerically on an (R,α) grid with 1024×256 points with hyper-radius R ranging from 0 to 30 a.u. If we substitute the time t by an imaginary time then any initial state in F and R will relax into the state of lowest possible energy (for more details, see [12]). The ground-state energies obtained are presented in Table II together with the results of the usual HF approach, the hyperspherical method, and the exact energies.

By examining the predicted ground-state energies for all five one-dimensional two-electron systems, we conclude that the hyperspherical approach provides surprising accuracy. This accuracy seems even to increase with increasing electron correlation (decreasing Z). The hy-

perspherical method is accurate within 0.6% for the negative hydrogen ion, and the accuracy decreases slightly to 2.3% for the helium atom. Note that in the hydrogen ion the correlation of the two electrons is more important than it is in helium. When the nuclear charge becomes larger, the accuracy of the method (estimated by the values of the ground-state energy predicted) decreases to 2.5%, which is comparable to the HF method accuracy in (R,α).

The accuracy found for $Z=1$ in three spatial dimensions is also known to be excellent. Using the adiabatic approximation (only one-channel functions) for the 3D H^- ground level energy one obtains -0.5273 a.u. ($-0.5277\ldots$ a.u. is exact).

So far we have restricted our discussion to energies. In the following we will also analyze the eigenfunctions. We focus on the negative hydrogen ion and compare the spatial electron-density distribution of its ground state as computed in four different ways: through the approximate methods mentioned above and via the exact one. The logarithmic contour plots are presented in Fig. 5. For comparison we have included the contour plot of the exact ground state in Fig. 5(a). Figure 5(b) shows the state as computed by the hyperspherical approximation. The agreement between both states is especially impressive for larger values of the hyper-radius R. For smaller values of R the hyperspherical state develops two maxima, corresponding to both electrons localized on opposite sides of the nucleus. This illustrates again that the hyperspherical method can exaggerate the importance of electron correlation.

In order to make a supplementary evaluation of the quality of the hyperspherical state we have also calculated the expectation value of the (exact) Hamiltonian (2.6) in this state. The expectation value obtained was 0.69 a.u. which differs by only 5% from the exact value.

The HF wave function calculated in (x_1,x_2) coordinates [Fig. 5(c)] shows more correlation and gives a better approximation to the exact wave function than the HF ground-state wave function calculated in coordinates (R,α) [Fig. 5(d)]. The original two-electron Hamiltonian $H(x_1,x_2)$ can be decomposed into a sum of two one-electron Hamiltonians plus a correction term: $H(x_1)+H(x_2)+C(x_1,x_2)$. The optimum correction term $C(x_1,x_2)$ can depend on the state as well as on the coordinate system. Good values of the HF ground-state energies obtained in (x_1,x_2) indicate that the two-electron correction term $C(x_1,x_2)$ for the ground state is small. In the hyperspherical coordinates the corresponding correction term in $H_R(R)+H_\alpha(\alpha)+C(R,\alpha)$ seems to be larger. The α dependence of $V(R,\alpha)$ is very different at various values of R. This decreases the accuracy of the HF approximation in the hyperspherical coordinates. Indeed the HF-method assumption that the wave function has the form of a product of functions depending either on R or on α, $\Psi(R,\alpha)=R^{-1/2}F(R)G(\alpha)$, cannot give a good approximation to the exact ground-state wave function at all values of R. The radial wave function $F(R)$ has the wrong asymptotic behavior at small values of the hyper-radius: it tends to zero too fast such that the total wave function

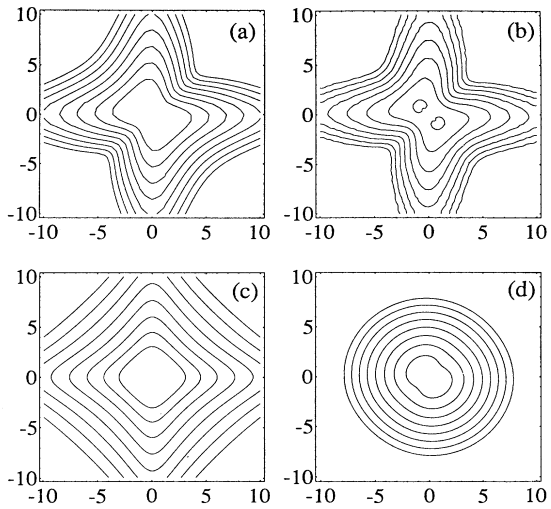

FIG. 5. Contour plot of the spatial distribution of the exact ground state $|\Psi_g(x_1,x_2)|^2$ of the negative ion ($Z=1$) compared to that calculated within three different approximation schemes. The eight contours shown in the figure correspond to $|\Psi_g(x_1,x_2)|^2=10^{-c}$, for $c=2,2.5,3,\ldots,5.5$. (a) Exact electron density distribution. (b) Hyperspherical approximation $|R^{-1/2}f(R)\Phi(R,\alpha)|^2$. (c) Hartree-Fock approximation $|g(x_1)g(x_2)|^2$. (d) Hyperspherically modified Hartree-Fock approximation $|R^{-1/2}F(R)G(\alpha)|^2$.

$\Psi(R,\alpha)=R^{-1/2}F(R)G(\alpha)$ is zero at the origin. The spatial distribution associated with the hyperspherical HF wave function has two shallow maxima corresponding to the two electrons located on the opposite sides of the nucleus.

The hyperspherical method, on the other hand, is based on adiabatic quasiseparability in R and α, and this is different from the HF assumption of complete independence in R and α. Let us also mention that the hyperspherical wave function gives the best agreement with the exact one. The qualitatively accurate representation of the atomic wave functions within the hyperspherical approach can be important for the collective response of the two electrons to the action of light. We hope to return to this topic in the future.

V. DISCUSSION AND CONCLUSIONS

We have tested whether the hyperspherical approach can be applied for reduced-dimensional two-electron systems. We have compared several hyperspherical energies for various 1D atoms and ions with their exact values, and found that this method works and that it even gives a remarkable accuracy. The applicability of the hyperspherical approach to one-dimensional systems is suggested by the symmetry properties with respect to parity and electron permutation. It follows from these symmetries that those potential curves which might contrib-

ute to the nonadiabatic coupling are separated by at least three other potential curves and have different asymptotic behavior at both small and large values of hyper-radius R. This suggests that each potential curve is only weakly coupled to other potential curves.

The results for the ground-state energies indicate interesting features of the hyperspherical method in one spatial dimension: the accuracy of the hyperspherical method increases with the increase of electron-electron correlation, or equivalently, with the decrease of the nuclear charge Z. This feature is opposite to the behavior of HF-like calculations in 1D which are more accurate for ground-state energies of atoms with $Z \geq 2$. We also compared the spatial distribution of the ground state obtained within different approaches, and found that the hyperspherical method exaggerates the profile shaping of the ground-state wave function associated with the electron correlation. To the contrary, the Hartree-Fock-like methods provide the wave functions with a rounder shape than it should have. We conclude that the hyperspherical method and the Hartree-Fock method are complementary to each other in the shape of the probability distribution they produce and in their applicability.

We also compared two versions of the HF approximation scheme: one applied in polar and the other one in Cartesian coordinates. The (x_1,x_2) form of the HF approach gives a better approximation to ground-state energies and wave functions than its polar coordinate version. This suggests that the Hamiltonian is less separable for the ground state in polar coordinates than in Cartesian coordinates.

The overall good reliability of the hyperspherical approximation in one dimension justifies a further exploration of 1D two-electron systems into regions of very high-lying singly and doubly excited states for which exact numerical computations are beyond the present capabilities of supercomputers. This approach might prove quite valuable especially in studies of strong-field interactions in which the induced level shifts and widths exceed the error uncertainty due to the hyperspherical approximation. We will return to this project in another note.

ACKNOWLEDGMENTS

We would like to thank S. L. Haan and M. V. Fedorov for many useful discussions and M. Kalinski for his constant help with MATHEMATICA. A. A. acknowledges the support of the National Science Foundation Grant No. PHY94-08733, as well as partial financial support from the Sloan Foundation. R.G. and J.H.E. acknowledge support by the Division of Chemical Sciences, Office of Basic Energy Sciences, Office of Energy Research of the U.S. Department of Energy.

[1] M. J. Seaton, Proc. Phys. Soc. **88**, 801 (1966); R. D. Cowan, *The Theory of Atomic Structure and Spectra* (Stanford University Press, Stanford, 1981); M. J. Seaton, Rep. Prog. Phys. **46**, 167 (1983).

[2] R. P. Madden and K. Codling, Phys. Rev. Lett. **10**, 516 (1963); Astrophys. J. **141**, 364 (1965).

[3] J. W. Cooper, U. Fano, and F. Prats, Phys. Rev. Lett. **10**, 518, (1963).

[4] T. F. O'Malley and S. Geltman, Phys. Rev. A **137**, 1344 (1965); P. L. Atick and E. N. Moore, Phys. Rev. Lett. **15**, 100 (1965); L. Lipsky and A. Russek, Phys. Rev. **142**, 59 (1966).

[5] J. Macek, J. Phys. B **1**, 831 (1968).

[6] A. D. Klemm and S. Ylarsen, Few-Body Systems **9**, 123 (1990).

[7] G. H. Hatton, Phys. Rev. A **14**, 901 (1976); J. E. Hornos, S. W. MacDowell, and C. D. Caldwell, *ibid.* **33**, 2212 (1986); V. V. Gusev, V. I. Puzynin, V. V. Kostrikin, A. A. Kvitinsky, S. P. Merkuriev, and L. P. Ponomarev, Few Body Systems **9**, 137 (1990); V. V. Kostrikin and A. A. Kvitinsky, J. Math. Phys. **35**, 47 (1994).

[8] U. Fano, Rep. Prog. Phys. **46**, 97 (1983).

[9] C. D. Lin, Adv. At. Mol. Phys. **22**, 77 (1986).

[10] H. Klar, P. Zoller, and M. V. Fedorov, Phys. Rev. A **30**, 658 (1984).

[11] A. G. Abrashkevich and M. Shapiro, Phys. Rev. A **50**, 1205 (1994).

[12] For some details of computational techniques used in obtaining exact two-electron wave functions, energies, spectra, etc., see R. Grobe and J. H. Eberly, Phys. Rev. A **48**, 4664 (1993).

[13] M. S. Pindzola, D. C. Griffin, and C. Bottcher, Phys. Rev. Lett. **66**, 2305 (1991).

[14] R. Grobe and J. H. Eberly, Phys. Rev. Lett. **68**, 2905 (1992).

[15] R. Grobe and J. H. Eberly, Phys. Rev. A **47**, RC1605 (1993).

[16] R. Grobe and J. H. Eberly, Laser Phys. **3**, 323 (1993).

[17] K. Rzazewski, M. Lewenstein, and P. Salieres, Phys. Rev. A **49**, 1196 (1994).

[18] B. Ritchie, Laser Phys. **3**, 355 (1993).

[19] G. S. Esra, K. Richter, G. Tanner, and D. Wintgen, J. Phys. B **24**, L413 (1991).

[20] S. L. Haan, R. Grobe, and J. H. Eberly, Phys. Rev. A **50**, 378 (1994).

[21] R. Grobe and J. H. Eberly, Phys. Rev. A **48**, 623 (1993); R. Grobe and S. L. Haan, J. Phys. B **27**, L735 (1994).

[22] R. Grobe, K. Rzazewski, and J. H. Eberly, J. Phys. B **27**, L503 (1994).

[23] J. Javanainen, J. H. Eberly, and Q. Su, Phys. Rev. A **38**, 3430 (1988). For a review, see J. H. Eberly, R. Grobe, C. K. Law, and Q. Su, in *Atoms in Strong Laser Fields,* edited by M. Gavrila, (Academic, Orlando, 1992), p. 323.

[24] For a review of time-dependent variational method, see A. K. Kerman and S. E. Koonin, Ann. Phys. **100**, 332 (1976).